PB90-116567

Statistical Comparison of the Effect of Relative and Absolute Humidity on Fixed-Bed Carbon Adsorption Capacity

Arkansas Univ., Fayetteville

Prepared for:

Environmental Protection Agency, Research Triangle Park, NC

1989

U.S. Department of Commerce
National Technical Information Service
NTIS

AEERL-P-542

TECHNICAL REPORT DATA
(Please read Instructions on the reverse before complet

1. REPORT NO. EPA/600/D-89/183	2.	3. PB90-116567
4. TITLE AND SUBTITLE A Statistical Comparison of the Effect of Relative and Absolute Humidity on Fixed-bed Carbon Adsorption Capacity		5. REPORT DATE 6. PERFORMING ORGANIZATION CODE
7. AUTHOR(S) J. E. Dunn (Univ. of Arkansas), and C. Nunez and M. Kosusko (EPA/AEERL)		8. PERFORMING ORGANIZATION REPORT NO.
9. PERFORMING ORGANIZATION NAME AND ADDRESS The University of Arkansas Department of Mathematics, Science and Statistics Fayetteville, Arkansas 72701		10. PROGRAM ELEMENT NO. 11. CONTRACT/GRANT NO. CR814945-01-0
12. SPONSORING AGENCY NAME AND ADDRESS EPA, Office of Research and Development Air and Energy Engineering Research Laboratory Research Triangle Park, NC 27711		13. TYPE OF REPORT AND PERIOD COVERED Published paper; 1/87 - 7/88 14. SPONSORING AGENCY CODE EPA/600/13

15. SUPPLEMENTARY NOTES AEERL project officer is Carlos M. Nunez, Mail Drop 61, 919/541-1156. Presented at 82nd Annual Meeting Air and Waste Management Association, Anaheim, CA, 6/25-30/89.

16. ABSTRACT The paper describes statistical methods used to evaluate data for toluene (at several typical operating temperatures and humidity levels) and to determine which measure of humidity (relative or absolute) is more important in determining carbon adsorption efficiency. The water content of a solvent-laden stream is critical for its control via carbon adsorption especially at relative humidities > about 50-70%. (Relative humidity is the percent of saturation; absolute humidity is the total water content.)

17. KEY WORDS AND DOCUMENT ANALYSIS

a. DESCRIPTORS	b. IDENTIFIERS/OPEN ENDED TERMS	c. COSATI Field/Group
Pollution	Pollution Control	13B
Carbon	Stationary Sources	07B
Adsorption	Relative Humidity	14G
Humidity	Absolute Humidity	04B
Statistics		12A
Toluene		07C

REPRODUCED BY
U.S. DEPARTMENT OF COMMERCE
NATIONAL TECHNICAL INFORMATION SERVICE
SPRINGFIELD, VA. 22161

18. DISTRIBUTION STATEMENT Release to Public	19. SECURITY CLASS *(This Report)* Unclassified 20. SECURITY CLASS *(This page)* Unclassified	21. NO. OF PAGES 27 22. PRICE

EPA Form 2220-1 (9-73)

NOTICE

This document has been reviewed in accordance with U.S. Environmental Protection Agency policy and approved for publication. Mention of trade names or commercial products does not constitute endorsement or recommendation for use.

89-29.1

EPA/600/D-89/183

A STATISTICAL COMPARISON OF THE EFFECT OF RELATIVE AND ABSOLUTE HUMIDITY ON FIXED-BED CARBON ADSORPTION CAPACITY

by

James E. Dunn
Department of Mathematics, Science and Statistics
University of Arkansas
Fayetteville, Arkansas 72701

and

Carlos Nunez and Michael Kosusko
U. S. Environmental Protection Agency
Air and Energy Engineering Research Laboratory
Research Triangle Park, North Carolina 27711

For Presentation at:
82nd Annual Meeting
Air and Waste Management Association
Anaheim, California June 25-30, 1989

INTRODUCTION

Adsorption is a technique that has been broadly applied for many years in the separation of substances from either gaseous or liquid streams. It involves the selective separation of compounds from a fluid phase onto the surface of a solid substrate known as the adsorbent. Activated carbon is generally the adsorbent of choice. In particular, activated carbon is effective in air pollution control.

In air pollution control applications, a solvent-laden air stream is passed through an activated carbon bed before it is vented to the atmosphere. In time, the bed will no longer adsorb the solvent; the air flow will need to be sent to a second bed; and the first bed will be regenerated, usually with steam. Air pollution control applications are typically driven by economics. One of the key factors in the economics is length of time a bed stays in operation between regenerations. This is related directly to the adsorption capacity of the carbon bed.

The moisture content of the solvent-laden stream is a critical parameter for its control by carbon adsorption and for the capacity of the bed. The higher the moisture content in general, the shorter the useful life of the bed between regenerations. The time until some specified *percent breakthrough* often is taken as a measure of performance of a carbon bed. For example, the 50 percent breakthrough time is the time required until the outlet concentration of gas is 50 percent of the inflow concentration (assuming a constant inflow rate).

The question to be answered here is whether it is *relative* humidity (RH) or *absolute* humidity (H_a) which is more critical to the degradation of the effectiveness of a carbon bed. In the absence of clear-cut guidance from the literature on choosing between the two, we propose:

Between RH and H_a, the more fundamental moisture measurement is the one that functions more independently of temperature with respect to determining the breakthrough curve.

This criterion does not deny the physical dependence of both *RH and H_a* on temperature. Its focus is on a comparison of the simple additivity of effects when jointly varying either temperature and RH, or temperature and H_a. Of necessity, our arguments will be statistically based on the data developed in AEERL's carbon adsorption laboratory, since no theory has been advanced as a guide to answer this question.

PRELIMINARY RESULTS

As a result of preliminary analysis of the breakthrough curves for carbon bed adsorption, two facts became evident. First, a relatively simple analysis of the time required to attain some standard feature, say 50 percent breakthrough, would not suffice. There simply were too many paths leading to (nearly) identical 50 percent breakthrough times to allow distinguishing the

necessarily subtle differences between the effects of RH and H_a. Thus, our reasoning led to a more fundamental approach, namely that of attempting to relate humidity effects to the parameters of a model for gaseous transport in adsorption beds.

The second fact that was discovered was that the familiar, symmetric sigmoid curve model, corresponding to the cumulative distribution function (c.d.f.) of a normal distribution, was inadequate. Once into the rise of the breakthrough curve, the transport process often would appear to "finish"; i.e., rise from 30 to 50 percent breakthrough more quickly than could be accounted for by this model. A transport model suggesting the normal c.d.f. is the Wiener diffusion process with non-zero infinitesimal drift, and possibly an absorbing barrier at the downstream bed/air interface. However, physical considerations argue against the Wiener process. It is a model for movement, whereas the dominant feature of adsorption beds is adsorption. Therefore, we undertook the development of a new transport model, based on first principles, whose properties evolve from the possibility of adsorption of a gas molecule on any one of a finite number of adsorption sites.

A "PARKING GARAGE" TRANSPORT MODEL

Suppose that a carbon bed is analogous to a large parking garage with a total of n_0 empty adsorption sites (analogous to parking spaces) available for occupancy at time $t = 0$. Continuing the analogy, also suppose that only the general path of travel for a molecule (analogous to an automobile) is defined between definite entry and exit points. Let ε denote the probability that an introduced molecule will occupy any particular empty site, and let n_t denote the number of occupied sites at time t. However, due to varying "parking practices," some multiple, say $1/\theta$, of the $n_0 - n_t$ available adsorption sites are "attractive" at time t. At this point, we will require only that $\theta > 0$ so that $0 < \theta < 1$ corresponds to the possibility of multiple adsorptions at the same site.

Let P(t) denote the probability that a molecule introduced at the entry at time t ultimately will pass through the exit. Assuming that the molecule attempts to occupy each site independently of all other sites, then from first principles governing independent events,

$$P(t) = (1 - \varepsilon)^{(n_0 - n_t)/\theta} \tag{1}$$

or in the form we shall use more frequently,

$$P(t)^{\theta} = (1 - \varepsilon)^{(n_0 - n_t)} \tag{2}$$

The initial value condition,

$$P(0)^{\theta} = (1 - \varepsilon)^{n_0}, \tag{3}$$

is immediate, and the boundary condition,

$$\lim_{\varepsilon \to 0} P(t) = 1 \ , \ t \geq 0, \tag{4}$$

is implied. By differentiating the logarithm of equation (2), we arrive at

$$P(t)^{-\theta} \frac{dP(t)^{\theta}}{dt} = - n'_t \ln(1 - \varepsilon) \tag{5}$$

Now consider the change in the number of occupied sites in a short time interval, Δt. We propose that

$$n_{t+\Delta t} - n_t \equiv \lambda \Delta t \left[1 - P(t)^{\theta}\right] , \tag{6}$$

where λ is proportional to the gas concentration, c_g (i.e., $\lambda = K c_g$, $K > 0$) and the term in brackets is a function of the probability of capture. Dividing by Δt and taking the limit as $\Delta t \rightarrow 0$, we obtain

$$n'_t = \lambda \left[1 - P(t)^{\theta}\right] \tag{7}$$

Substitution of equation (7) in equation (5) results in

$$\frac{dP(t)^{\theta}}{P(t)^{\theta}\left[1-P(t)^{\theta}\right]} = -\lambda \ln(1 - \varepsilon) dt \ , \tag{8}$$

with solution

$$P(t) = \left[1 + C^{-1} e^{\lambda t \ln(1 - \varepsilon)}\right]^{-1/\theta} , \tag{9}$$

where choice of

$$C = (1 - \varepsilon)^{n_0}/\left[1 - (1 - \varepsilon)^{n_0}\right] \tag{10}$$

allows both conditions (3) and (4) to be satisfied.

Equation (9) is known most widely as a *generalized logistic growth law,*[1] the generalization being that of allowing $\theta \neq 1$. We shall refer to equation (9) as the *parking garage* (PG) transport model. For our purposes, it is most useful to solve this equation for t to obtain the model

$$t = \alpha + \beta \ln[P^{\theta}/(1 - P^{\theta})], \tag{11}$$

expressing the time to breakthrough as a function of the breakthrough fraction, P, where

$$\alpha = - \ln(C)/[- \lambda \ln(1 - \varepsilon)] , \tag{12}$$

$$\beta = [(\lambda \ln(1 - \varepsilon)]^{-1} . \tag{13}$$

The parameters used in the PG transport model are summarized in Table 1.

Properties of the Model

Since the parameter β reflects how fast t will change over the range of P, $0 < P < 1$, β controls the general slope of the curve. A low value of β, corresponding to a high gas concentration, or ε close to 1, will result in a sharp rate of ascent; a high value of β corresponding to a low gas concentration, or ε close to 0, will result in a rather flat breakthrough curve. This is illustrated in Figure 1. Values $\hat{\alpha} = 116.9$, $\hat{\beta} = 6.480$, and $\hat{\theta} = 1.5743$ were obtained as the geometric means of separate estimates obtained for eight replications of carbon bed absorption (Table 2, runs S02 - 54), which were challenged with a concentration of 1000 ppm toluene at 29.4 °C and 50 percent RH. Plots are increasingly steep as β is varied from 1.4 $\hat{\beta}$, through $\hat{\beta}$, to 0.6 $\hat{\beta}$, while holding constant $\hat{\alpha} = 116.9$ and $\hat{\theta} = 1.5743$.

For plots of this form in which only β is varied, the *fixed point* at the intersection of the curves is at the coordinate $(t_F, P_F) = (\alpha, 2^{-1/\theta})$. Below the *fixed point*, breakthrough occurs sooner for a curve with a small slope, while above the *fixed point*, breakthrough occurs sooner for a steep curve.

Equation (11) suggests that the breakthrough curve translates linearly to the right or left with the parameter α. However, equation (12) clearly shows that α is functionally related to β as a result of their joint dependence on λ and ε, thus putting the physical existence of the *fixed point* in question. Clearly, the entire curve must shift to the left with increasing slope as λ increases in response to increasing c_g, and conversely. However,

from equation (10), it is evident that for large n_0,

$$C \equiv (1-\varepsilon)^{n_0}, \tag{14}$$

and thus, to a good approximation,

$$\alpha \approx n_0/\lambda = n_0/(K\ c_g). \tag{15}$$

Figure 2 illustrates the rapid rate of convergence of $\log_{10}(\alpha)$ to the $\log_{10}(n_0/\lambda)$ limiting curve for ε = 0.1, 0.01, and 0.001, and λ = 1. On a logical basis, even if ε is very small, one would expect that a typical molecule would encounter far more than 10,000 adsorption sites in its passage through a regenerated carbon bed. Therefore, for fixed c_g, we conclude that a breakthrough curve translates not only linearly with α, but essentially independently of β as well. The *fixed point* represents an ε-invariant, physical reference point with abscissa proportional to n_0/c_g. Empirical evidence for independence of the scaled parameters

$$\alpha_s = \alpha \times c_g \approx n_0/K\ , \text{ and} \tag{16}$$

$$\beta_s = \beta \times c_g = [-K \ln(1-\varepsilon)]^{-1} \tag{17}$$

are presented under Parameter estimation.

Equating the second derivative of equation (9) to 0 yields the coordinates of a single *inflection point*, $(t_P, P_I) = [\alpha - \beta \ln(\theta), (1+\theta)^{-1/\theta}]$, on the breakthrough curve. Clearly, this coordinate is identical to that of the *fixed point* if $\theta = 1$. If $\theta < 1$, then the *inflection point* occurs later ($t_F < t_I$) and higher ($P_F < P_I$) than the *fixed point;* the converse being true when $\theta > 1$. Figure 1, with fixed point at (116.9, 0.6439), illustrates the latter case. Inflection points occur at a common ordinate of 0.5485, and abscissas of 115.1, 114.0, and 112.8 corresponding to 0.6β, β, and 1.4β, respectively. P_I is not infinitely variable, however, being bounded by $e^{-1} \approx 0.368$ as $\theta \to 0$, and above by 1 as $\theta \to \infty$.

Figure 3 illustrates the effect of varying θ through $0.5\,\hat{\theta}$, $\hat{\theta}$, and $2\,\hat{\theta}$, while holding constant $\hat{\alpha}$ = 116.9 and $\hat{\beta}$ = 6.480. Recalling that $1/\theta$ represents the fraction of empty adsorption sites which are "attractive," the curve corresponding to $\theta = 0.5\,\hat{\theta} = 0.787$ represents the situation where as many as 1/0.787 = 1.27 molecules might occupy an average adsorption site. By

contrast, the curve corresponding to $\theta = 2\hat{\theta} = 3.15$ represents the situation where only 1/3.15 = 0.317 of the available sites are "attractive" for molecular adsorption. Increasing "attractiveness" results in both an extended time to breakthrough and a greater rate of change once breakthrough has occurred. Even though θ relates to both translation and slope properties of breakthrough curves, because it solely determines the ordinates of *fixed* and *inflection points*, it will be referred to here as the "shape" parameter.

Parameter estimation

Table 2 lists the time in minutes until 10, 20, 30, 40, and 50 percent breakthrough for 52 test runs using two beds, A and B, which were challenged with toluene. Toluene concentrations were 200 and 1000 ppm, with separate runs being made at 29.4 and 48.9 °C, and with RH and H_a ranging over the values shown in Table 2. The breakthrough times shown there are not strictly direct measurements. In 30 percent of the cases, considerable smoothing of the original output concentrations was necessary in order to avoid what appeared to be extraneous, minor peaks and troughs.[2]

Least squares estimates of the parameters α, β, and θ were obtained using SAS procedure NLIN and the model defined by equation (11). Convergence of the least squares iteration generally was quick and reliable, probably because the model is linear α and β.

Estimates of parameters and of certain derived properties are summarized in Table 3. Fits to the data points in Table 2 were excellent in every case, as reflected by individual root mean squared errors (RMSE) shown in Table 3. For comparison's sake, the standard deviation of replications in times until 50 percent breakthrough among identical temperature/concentration/ RH/bed combinations was estimated to be 13.6 minutes.

Independence of α_s and β_s

As verification of the asymptotic assumption leading to equation (15), we obtained the following correlations among estimates $\hat{\alpha}_s$, $\hat{\beta}_s$, and $\hat{\theta}$ after adjusting out mean differences attributable to concentration, temperature, RH, and bed differences:

	Correlation	p-value
$\hat{\alpha}_s$ vs $\hat{\beta}_s$	-0.0346	0.876
$\hat{\alpha}_s$ vs $\hat{\theta}$	-0.0815	0.712
$\hat{\beta}_s$ vs $\hat{\theta}$	-0.508	0.013

From the lack of significance of the correlation between $\hat{\alpha}_s$ and $\hat{\beta}_s$, it is evident that α_s and β_s have been released from their joint dependence on ε. Further, lack of significance of the correlation between $\hat{\alpha}_s$ and $\hat{\theta}$ suggests that the breakthrough curves translate freely to the right or left, at least among replications, in response to changing α_s regardless of the values of β_s and θ. Lack of independence between $\hat{\beta}_s$ and $\hat{\theta}$ suggests that slope is not independent of the point of inflection, at least in a statistical sense, even though β_s and θ are mathematically independent parameters. Physically, one might expect that the probability of adsorption is related to the "attractiveness" of a site.

THE ROLE OF HUMIDITY

In the absence of any theory with which to relate the PG model parameters to physical conditions of the experiments, we resorted to the use of empirical, polynomial models based on traditional multiple regression methods. In order to guarantee that the fitted models would be physical, all analyses involved natural logarithms of estimates $\hat{\alpha}_s$ and $\hat{\theta}$, shown in Table 3 as response variables. $\hat{\beta}_s$ was not transformed since it is already expressed in units of $\ln(1 - \varepsilon)$.

Based on preliminary analyses, we narrowed the search for possible exp'anatory variables to:

Main effects:	*Interaction effects:*
TEMP = temperature, °C,	CONC x TEMP,
CONC = ppm toluene concentration,	BED x TEMP,
BED = 0 if Bed A, 1 if Bed B,	BED x CONC.
Effects involving RH:	*Effects involving* H_a:
RH = percent relative humidity,	H_a = percent absolute humidity,
RH^2, CONC x RH, RH x BED,	H_a^2, CONC x H_a, H_a x BED,
TEMP x RH, TEMP x RH^2.	TEMP x H_a, TEMP x H_a^2

Since the ultimate goal was to distinguish between the effects of RH and H_a, any model examined always consisted of a subset of the main effects, the interaction effects, and the effects involving either RH or H_a.

Our general approach was to use SAS procedure RSQUARE to arrive at a "best" model in terms of maximum R^2 without allowing use of temperature x RH interactions, then to repeat the model selection while making these

interactions available. The following three criteria, suggested by Draper and Smith,[3] were used in model selections:

(1) Minimum mean squared error (MSE).

(2) Mallow's C_P statistic. The ideal model corresponds to both a small C_P and one which is approximately equal to the number of predictors in the models including the intercept.

(3) Lack of fit, compared to an estimate of pure error variance, based on replications of temperature/concentration/RH/bed combinations. Estimates of pure error variances were 0.216 (22 d.f.) for $\ln(\hat{\alpha}_s)$, 7.36×10^6 (22 d.f.) for $\hat{\beta}_s$, and 0.316 (20 d.f.) for $\ln(\hat{\theta})$.

Prediction of α_s

By our definition and based on model comparisons which are summarized in Table 4, the evidence points to RH as being more fundamental than H_a in determining α_s, the parameter which reflects the number, n_0, of adsorption sites and the extent of horizontal translation of the *fixed point* of a breakthrough curve. Figure 4 shows a plot of C_P statistics for maximum R^2 models containing 5 - 11 terms, including the intercept. Solid curves correspond to allowing temperature x RH interactions to be selected as predictors; dashed curves indicate the results of excluding these interactions from the selection list. Figure 5 shows analogous curves for the MSE criterion. In every case, C_P curves attained their minimums at the next integer value after crossing the reference line, $C_P = p$. Note that these same integers also correspond to the locations of "elbows" in the MSE curves where their respective minimums were first attained. Therefore, the evidence is strong that these integers represent an optimal number of predictors in the respective models. Actual predictors for the maximum R^2 of Models 1 - 4, corresponding to these integers, are listed in Table 4.

Even though Model 2, with temperature x RH interactions excluded, requires one additional term compared to Model 1, both models attain nearly identical values of R^2 and MSE. We interpret this as indicating that temperature x RH interactions can play a surrogate role for other variables in a model based on RH. In fact, Model 2 gives a slightly better fit than Model 1 using pure error as a criterion.

Model 3, based on temperature x H_a interactions, required still one additional predictor but attained essentially the same R^2 and MSE as Models 1 and 2. Again, the surrogate role of H_a and its temperature interactions appears to be in effect. However, in the absence of temperature x H_a interactions, Model 4 could not attain the previous levels of MSE based on H_a alone. It appears that explicit temperature x H_a interactions are required in

order for H_a to assume a surrogate role for RH. Finally, while addition of temperature x RH interactions to Model 2 did not cause a significant improvement in model fit ($p = 0.3292$), a significant improvement ($p = 0.0570$) was obtained for Model 4 by addition of temperature x H_a interactions.

Prediction of β_s

Though less compelling than that for α_s, the evidence indicates that RH is more fundamental than H_a in determining β_s, the parameter which determines ε, the probability of adsorption at a site, and the general slope of a breakthrough curve. Maximum R^2 models for prediction of β_s are compared in Table 5. Notice that predicted values, $\hat{\alpha}_{s1}$, ..., $\hat{\alpha}_{s4}$, obtained from Models 1 - 4 defined in the above section for α_s and their logarithms, were added to the selection list of potential predictors. For comparable numbers of predictors, maximum R^2 was increased by 18.7 percent for Model 2 and 6.5 percent for Model 3 through use of these estimates. Models 1 and 4 were relatively indifferent to selection of $\hat{\alpha}_s$. The fact that these variables often were selected because of their relation to $\hat{\beta}_s$ does not contradict our discussion of the independence of α_s and β_s; a statistical relationship, originating from variations in experimental conditions, is reflected here.

As before, the optimal number of terms to be included in each prediction equation was determined from plots of C_p and MSE curves, shown as Figures 6 and 7, respectively. The results are quite analogous to those for $\ln(\hat{\alpha}_s)$. Models 1 - 3 attained essentially identical values for maximum R^2, C_p, and MSE. Model 2 may have a slight predictive advantage. Again, temperature x RH interactions appear to play a surrogate role in Model 1. Model 4, without access to temperature x H_a interactions, was incapable of attaining a comparable level of MSE. Even though all models gave an adequate fit, compared to the estimate of pure error variance, and neither Model 2 nor Model 4 showed a significant improvement when temperature x RH interactions were added, we attribute this lack of discrimination to the poor reproducibility of estimates of β_s. This is evident from replicated estimates of β_s shown in Table 3, and from the relatively low values of R^2 obtained here compared to those for $\ln(\hat{\alpha}_s)$.

Predictions of θ

Even though runs 305 - 307 suggested that high values of $\hat{\theta}$ were reproducible, runs 19 and S02 were excluded as potential outliers, based on a comparison with their replicates. This resulted in a 50 percent reduction in the estimate of pure error variance.

Table 6 compares maximum R^2 models for prediction of $\ln(\theta)$. Predicted values $\hat{\beta}_{1s}, \ldots, \hat{\beta}_{4s}$ were added to the selection list which already contained $\hat{\alpha}_{si}$ and $\ln(\hat{\alpha}_{si})$, i = 1,.., 4. In this instance, C_P failed as a guide to the proper number of predictors, generally assuming only negative values. The optimal number was chosen from the plot of MSE curves shown as Figure 8. Again Model 4 seemed incapable of attaining MSE at a level comparable to those for Models 1 - 3. Model 2, without access to temperature x RH interactions, has the same predictive advantage as Model 1. All models suffered from poor fits, as reflected by small R^2 and as compared to the estimate of pure error, but adding temperature x RH interactions to Models 2 and 4 did not significantly improve their fits.

Perhaps it is too much to expect discrimination among competing models with respect to a parameter which in half the cases determines an unmeasured value above and beyond the 50 percent breakthrough point. Nevertheless as before, the evidence suggests a more fundamental role for RH than H_a in the determination of θ, and thus of P_I and P_F, and ultimately the "attractiveness" of the adsorption sites for toluene. An examination of estimated θ values in Table 3 suggests a range of variability from 0.059 to 12 as the multiple of the number of available sites which are "attractive" for adsorption.

DISCUSSION AND CONCLUSIONS

Based on a pragmatic definition, RH has emerged as a more fundamental quantifier of the effects of moisture on carbon bed adsorption of toluene than H_a. As a means of reaching this empirical conclusion, we have developed a theoretical model which relates time to fraction of breakthrough and those parameters are physically interpretable. In particular, the model suggests a new reference point on the time axis. This is a *fixed point* whose abscissa is determined by the ratio of initially available adsorption sites to the concentration of the challenging gas, whose ordinate is determined by the multiple of these sites which are attractive, and which is invariant with respect to changes in the basic probability of adsorption of a molecule at any particular site. As such, the *fixed point* seems superior to the more familiar *inflection point*, which traditionally has been assumed to occur at the time of 50 percent breakthrough. Our estimates indicate that, depending on experimental conditions, inflection may occur at as low as 38 percent and as high as 83 percent breakthrough.

In our search for best empirical models to account for variation in the PG model parameters, bed differences and their interactions with other physical variables of the experiment frequently appeared. This is difficult to explain, but it seems better to have accounted for these differences in our examination of the relative roles of RH and H_a than to have ignored them.

For interpolation purposes, the fitted forms of Model 2 are:

$$\ln(\hat{\alpha}_{s2}) = 13.4264 - 1.55209 \times 10^{-3} \text{ Concentration (ppm)}$$
$$- 2.05133 \times 10^{-4} \text{ RH}^2 \text{ (percent}^2\text{)}$$
$$+ 3.0009 \times 10^{-5} \text{ Concentration x RH}$$
$$- 4.12487 \times 10^{-2} \text{ Temperature (°C)}$$
$$- 1.80743 \times 10^{-2} \text{ RH (percent)}$$
$$+ 1.43867 \times 10^{-1} \text{ BED (0 if bed A, 1 if bed B)}$$
$$+ 2.5326 \times 10^{-5} \text{ Concentration x Temperature.}$$

$$\hat{\beta}_{s2} = -149214 + 1.71946 \times 10^{4} \ln(\hat{\alpha}_{s2})$$
$$- 4.22419 \times 10^{-1} \hat{\alpha}_{s2}$$
$$- 4.29204 \times 10^{-1} \text{ Concentration x Temperature}$$
$$- 1.75285 \text{ RH}^2$$
$$+ 1.94981 \times 10^{1} \text{ Concentration.}$$

$$\ln(\hat{\theta}) = 1.96417 - 2.38724 \times 10^{-4} \hat{\beta}_{s2}$$
$$- 2.24874 \times 10^{-4} \text{ RH}^2$$
$$+ 1.4711 \times 10^{-5} \text{ Concentration x RH}$$
$$- 7.73738 \times 10^{-3} \text{ Temperature x Bed.}$$

In applications, one must obtain $\hat{\alpha} = \hat{\alpha}_{s2}$ x concentration and $\hat{\beta} = \hat{\beta}_{s2}$ x concentration. Substitution of both Bed = 0 and Bed = 1 will suggest the range of variability to be anticipated among beds. The complexity of the physical relationships implied by the above models can begin to be understood if one identifies each predictor with its corresponding partial derivative. For example, the presence of RH^2 in the second equation would suggest the requirement for $\partial^2\beta_s/\partial RH^2$ in any mechanistic model.

Table 1. Relations among the parameters of the PG transport model.

Fundamental parameters:

c_g = gas concentration,

λ = concentration intensity, $\lambda = \kappa \times c_g$ assumed with $\kappa > 0$,

n_0 = number of adsorption sites available at time t= 0,

ε = probability of adsorption at any open site, $0 < \varepsilon < 1$,

$1/\theta$ = fraction of available sites which are "attractive", $\theta > 0$.

Operational parameters:

$C = (1 - \varepsilon)^{n_0}/[1 - (1 - \varepsilon)^{n_0}]$, the integration constant,

$\alpha = - \ln(C)/[- \lambda \ln(1 - \varepsilon)]$, the "intercept," and ε-invariant *fixed point* abscissa,

$\simeq n_0/\lambda = n_0/(\kappa \times c_g)$ as $n_0 \to \infty$,

α_s $\alpha \times c_g \simeq n_0/\kappa$, the "scaled intercept,"

$\beta = [- \lambda \ln(1 - \varepsilon)]^{-1}$, the "slope," $\beta > 0$,

β_s $\beta \times c_g = [- \kappa \ln(1 - \varepsilon)]^{-1}$, the "scaled slope."

Derived relations:

$C = \exp(-\alpha/\beta)$,

$P(0) = [C/(1 + C)]^{1/\theta} = [1 + \exp(\alpha/\beta)]^{-1/\theta}$, $0 < P < 1$,

t_I = time at inflection (t_I satisfies $d^2P/dt^2 = 0$)

$= \alpha - \beta \ln(\theta)$,

P_I = fraction of breakthrough at the time of inflection

$= (1 + \theta)^{-1/\theta}$, $e^{-1} < P_I < 1$.

Table 2. Test conditions and observed times to specified breakthrough percentages.

Run	CONC	TEMP	RH	W(ABS)	Bed	10%	20%	30%	40%	50%
						(minutes)				
07	200	29.4	30	0.0076	A	449.0	486.3	511.0	529.8	---
08	200	29.4	30	0.0076	B	428.8	452.7	467.7	478.5	488.3
39	200	29.4	70	0.0183	A	112.5	125.0	135.7	143.0	---
41	200	29.4	70	0.0183	A	114.3	130.8	143.3	153.3	163.5
17	200	48.9	70	0.0550	A	34.8	42.8	46.8	51.0	53.8
19	200	48.9	70	0.0550	A	41.5	48.5	52.5	55.5	57.5
18	200	48.9	70	0.0550	B	60.8	59.3	63.7	67.0	70.0
20	200	48.9	70	0.0550	B	62.0	70.7	76.7	81.0	85.5
90	1000	29.4	0	0.0000	A	83.8	92.7	98.0	104.8	110.8
91	1000	29.4	0	0.0000	B	108.8	114.7	118.3	122.0	125.1
01	1000	29.4	30	0.0076	A	88.0	97.5	102.5	107.0	---
02	1000	29.4	30	0.0076	B	102.7	111.5	117.2	120.8	---
04	1000	29.4	30	0.0076	B	98.3	104.8	108.7	111.7	113.8
S01	1000	29.4	50	0.0130	A	71.0	82.0	89.5	95.2	99.0
S03	1000	29.4	50	0.0130	A	77.2	87.0	93.3	97.7	101.5
51	1000	29.4	50	0.0130	A	119.7	127.5	132.8	138.0	142.3
53	1000	29.4	50	0.0130	A	77.3	86.5	93.3	98.7	103.5
S02	1000	29.4	50	0.0130	B	92.5	100.0	105.0	108.1	109.5
S04	1000	29.4	50	0.0130	B	95.0	103.0	107.0	111.0	114.2
52	1000	29.4	50	0.0130	B	125.7	132.3	136.2	139.8	143.0
54	1000	29.4	50	0.0130	B	96.7	103.7	107.3	112.0	115.3
312	1000	29.4	60	0.0157	A	64.6	71.2	75.7	79.7	84.5
100	1000	29.4	70	0.0183	A	71.7	77.7	80.8	84.3	87.5
103	1000	29.4	70	0.0183	A	57.0	63.0	67.7	72.2	76.0
13	1000	29.4	70	0.0183	A	58.0	64.7	69.7	73.0	---
15	1000	29.4	70	0.0183	A	54.7	61.5	67.8	72.0	---
101	1000	29.4	70	0.0183	B	62.2	65.7	68.8	71.0	72.8
104	1000	29.4	70	0.0183	B	73.8	78.3	81.7	85.0	87.8
14	1000	29.4	70	0.0183	B	69.0	75.0	79.5	82.8	---
16	1000	29.4	70	0.0183	B	73.0	78.7	83.0	86.2	89.2
316	1000	29.4	80	0.0210	A	58.5	64.0	67.8	71.7	74.5
317	1000	29.4	80	0.0210	B	67.8	72.5	75.5	78.7	80.7
320	1000	29.4	90	0.0239	A	57.1	62.3	65.8	69.3	71.5
322	1000	29.4	90	0.0239	A	45.3	50.1	53.0	57.0	59.8
323	1000	29.4	90	0.0239	B	62.1	67.5	70.1	72.9	75.8
94	1000	48.9	0	0.0000	A	69.7	75.8	80.7	84.8	89.2
93	1000	48.9	0	0.0000	B	83.5	87.5	90.7	93.8	96.3
21	1000	48.9	30	0.0221	A	78.3	87.5	93.7	98.3	102.3
23	1000	48.9	30	0.0221	A	59.3	67.5	73.3	76.8	80.2
22	1000	48.9	30	0.0221	B	94.7	102.5	107.3	111.0	115.5
24	1000	48.9	30	0.0221	B	75.3	81.8	85.8	89.0	91.2
300	1000	48.9	60	0.0465	A	45.0	48.7	50.2	51.5	53.0
301	1000	48.9	60	0.0465	B	47.0	50.0	53.0	55.0	56.3
09	1000	48.9	70	0.0550	A	33.5	38.0	41.3	43.7	.
11	1000	48.9	70	0.0550	A	33.7	39.0	42.8	45.5	48.0
10	1000	48.9	70	0.0550	B	41.2	44.7	46.8	48.5	51.0
12	1000	48.9	70	0.0550	B	43.2	48.0	51.2	53.8	57.0
306	1000	48.9	80	0.0630	A	47.0	52.3	55.7	57.5	59.0
305	1000	48.9	80	0.0630	B	39.8	44.5	46.5	48.0	49.5
307	1000	48.9	80	0.0630	B	40.7	45.0	47.0	48.7	49.5
308	1000	48.9	90	0.0722	A	39.0	40.7	41.7	42.5	43.3
309	1000	48.9	90	0.0722	B	37.1	39.9	41.2	42.5	43.7

Table 3. Estimates of operational parameters and derived properties for the PG transport model.

Run	RMSE	Fixed Point $\hat{a} = t_F$	P_F	$\hat{\theta}$	$\hat{a}_s$	$\hat{\beta}_s$	P_0	Inflection t_I	P_I
07	0.418	561.526	0.586	1.2950	112305	7685.4	1.26E-6	551.6	0.527
08	0.205	506.429	0.700	1.9412	101286	3483.1	3.1E-7	494.9	0.574
39	0.917	130.610	0.250	0.5000	26102	4703.2	1.50E-5	146.8	0.414
41	0.268	139.193	0.266	0.5234	27839	5873.5	1.15E-4	158.2	0.447
17	0.251	60.019	0.899	1.9389	12004	1169.8	5.03E-3	56.1	0.574
19	0.121	64.535	0.960	16.9684	12907	117.7	1.56E-3	62.9	0.843
18	0.266	77.831	0.843	4.0507	15566	877.3	1.29E-3	73.8	0.670
20	0.196	86.802	0.533	1.1008	17360	2023.4	4.12E-4	85.8	0.509
90	0.616	51.057	0.001	0.0831	51057	21123.3	0.0	103.6	0.383
91	0.205	120.601	0.360	0.6792	120601	8852.7	0.0	124.0	0.466
01	0.391	118.286	0.749	2.3979	118286	5478.2	1.23E-4	113.5	0.400
02	0.277	132.592	0.812	3.3380	132592	3895.9	3.73E-5	127.9	0.644
04	0.116	120.100	0.807	3.2353	120100	2930.5	3.15E-6	116.7	0.640
S01	0.484	108.381	0.713	2.0496	108381	7966.2	1.31E-3	102.7	0.580
S03	0.137	109.774	0.730	2.2002	109774	6445.3	4.35E-4	104.7	0.589
S1	0.214	132.032	0.281	0.5465	132032	13345.7	1.0E-8	140.1	0.450
S3	0.216	100.220	0.432	0.8268	100220	13190.1	1.02E-4	102.7	0.482
S02	0.623	117.635	0.965	15.0105	117635	723.8	1.99E-5	115.7	0.831
S04	0.358	119.072	0.662	1.6826	119072	6222.9	1.15E-5	115.8	0.556
S2	0.168	143.375	0.513	1.0395	143375	7673.0	2.0E-8	143.1	0.504
S4	0.525	110.751	0.374	0.7053	110751	9946.2	1.4E-7	114.2	0.469
312	0.330	60.897	0.060	0.2459	60897	13909.7	2.0E-8	80.4	0.409
100	0.376	83.971	0.388	0.7312	83971	8231.4	8.7E-7	86.5	0.472
103	0.503	69.099	0.333	0.6303	69099	10307.2	2.40E-5	73.9	0.460
13	0.349	77.891	0.545	1.1413	77851	7809.3	1.60E-4	76.9	0.513
15	0.643	55.481	0.110	0.3136	554B1	15193.1	8.0EE-6	73.1	0.419
101	0.277	71.176	0.416	0.7893	71176	5622.3	8.0E-8	72.5	0.478
104	0.135	73.664	0.098	0.2984	73664	9663.2	0.0	85.3	0.417
14	0.218	83.539	0.420	0.7993	83539	8735.6	6.37E-6	85.5	0.480
16	0.162	87.902	0.456	0.8823	87902	7903.4	3.35E-6	88.9	0.488
316	0.276	67.940	0.299	0.5741	67940	9357.4	3.21E-6	73.1	0.454
317	0.294	79.606	0.450	0.8672	79606	6389.9	5.8E-7	80.5	0.487
320	0.319	70.731	0.465	0.9060	70731	8993.6	1.43E-5	71.4	0.491
322	0.420	37.071	0.016	0.1666	37071	10866.8	0.0	56.5	0.397
323	0.406	74.595	0.459	0.8899	74595	6475.5	2.39E-6	75.4	0.489
94	0.110	63.120	0.038	0.2116	63120	14119.8	0.0	86.0	0.404
93	0.186	81.150	0.062	0.2497	81150	9157.4	0.0	93.9	0.410
21	0.149	107.367	0.626	1.4783	107367	8638.3	2.23E-4	104.0	0.541
23	0.315	87.107	0.720	2.1098	87107	5748.3	7.60E-4	82.8	0.584
22	0.391	114.040	0.468	0.9124	114040	9769.6	2.78E-6	114.9	0.491
24	0.164	96.992	0.748	2.3824	96992	3963.8	3.46E-5	83.6	0.600
300	0.311	55.933	0.798	3.0752	55933	1528.1	6.77E-6	54.2	0.633
301	0.424	56.304	0.488	0.9870	56304	4463.3	2.18E-6	56.5	0.497
09	0.153	45.418	0.470	0.9189	45418	6007.1	2.87E-4	45.9	0.492
11	0.139	49.890	0.575	1.2521	49890	5742.9	9.70E-4	48.6	0.523
10	0.322	44.934	0.218	0.4552	44934	5925.5	6.08-8	49.6	0.439
12	0.242	49.448	0.246	0.4936	49448	8262.0	5.39E-6	55.3	0.444
306	0.289	64.418	0.952	14.0306	64418	536.1	1.91E-4	63.0	0.824
305	0.346	53.605	0.942	11.6215	53605	508.3	1.14E-4	52.4	0.804
307	0.331	53.607	0.954	14.8810	53607	371.0	6.07E-6	52.6	0.830
308	0.044	44.056	0.609	1.3981	44056	1586.8	0.0	43.5	0.585
309	0.168	45.321	0.663	1.6841	45321	2118.3	3.04E-6	44.2	0.556

Table 4. Comparisons of best regression models for prediction of $\ln(\alpha_s)$ with and without use of temperature x humidity interactions.

	Best RH models		Best H_a models	
	Temp. x RH interactions		Temp. x H_a interactions	
	Yes	No	Yes	No
	Model 1(α_{s1})	*Model 2*(α_{s2})	*Model 3*(α_{s3})	*Model 4*(α_{s4})
Predictors*	CONC, RH^2	CONC, RH^2	CONC, H_a^2	CONC, H_a
	CONC x RH	CONC x RH	CONC x H_a	CONC x H_a
	CONC x BED	CONC x TEMP	CONC x TEMP	CONC x TEMP
	TEMP x RH	TEMP, BED	TEMP, BED	TEMP, BED
	TEMP x RH^2	RH	TEMP x H_a	
			TEMP x H_a^2	
No. of terms*	7	8	9	7
R^2	0.896	0.896	0.899	0.840
C_p	5.39	6.83	6.69	4.34
MSE	0.0422	0.0429	0.0428	0.0647
p, lack-of-fit	0.0080	0.0232	0.0066	0.0002
p, due to TEMP x H and TEMP x H^2	---	0.3292	---	0.0570

* An intercept was included in every model.

Table 5. Comparisons of best regression models for prediction of β_s with and without use of temperature x humidity interactions.

	Best RH models		Best H_a models	
	Temp. x RH interactions		Temp. x H_a interactions	
	Yes	No	Yes	No
	Model 1(β_{s1})	*Model 2*(β_{s2})	*Model 3*(β_{s3})	*Model 4*(β_{s4})
Predictors*	$\hat{\alpha}_{s1}$, BED	$\hat{\alpha}_{s2}$, $\ln(\hat{\alpha}_{s2})$	$\hat{\alpha}_{s3}$, $\ln(\hat{\alpha}_{s3})$	H_a, BED
	CONC x RH	CONC x TEMP	CONC x H_a	CONC
	RH x BED	CONC, RH^2	H_a x BED	H_a x BED
	TEMP x BED		CONC, BED	
	TEMP x RH			
No. of terms*	7	6	7	5
R^2	0.632	0.647	0.636	0.590
C_p	5.60	4.46	3.80	0.00
MSE	8.04×10^6	7.56×10^6	7.97×10^6	8.59×10^6
p, lack-of-fit	0.350	0.455	0.363	0.261
p, due to TEMP x H and TEMP x H^2	---	0.841	---	0.981

* An intercept was included in every model.

Table 6. Comparisons of best regression models for prediction of ln(θ) with and without use of temperature x humidity interactions.

	Best RH models		Best H_a models	
	Temp. x RH interactions		Temp. x H_a interactions	
	Yes	No	Yes	No
	Model 1(θ_{s1})	*Model 2*(θ_{s2})	*Model 3*(θ_{s3})	*Model 4*(θ_{s4})
Predictors*	$\hat{\alpha}_{s1}$	$\hat{\beta}_{s2}$, RH^2	$\hat{\alpha}_{s3}$, $\ln(\hat{\alpha}_{s3})$	$\hat{\beta}_{s4}$
	CONC x RH	CONC x RH	CONC x H_a	CONC x H_a
	RH x BED	TEMP x BED		
	TEMP x RH			
No. of terms*	5	5	4	3
R^2	0.415	0.429	0.401	0.247
MSE	0.692	0.676	0.694	0.853
p, lack-of-fit	0.0056	0.0067	0.0057	0.0012
p, due to TEMP x H and TEMP x H^2	---	0.826	---	0.930

* An intercept was included in every model.

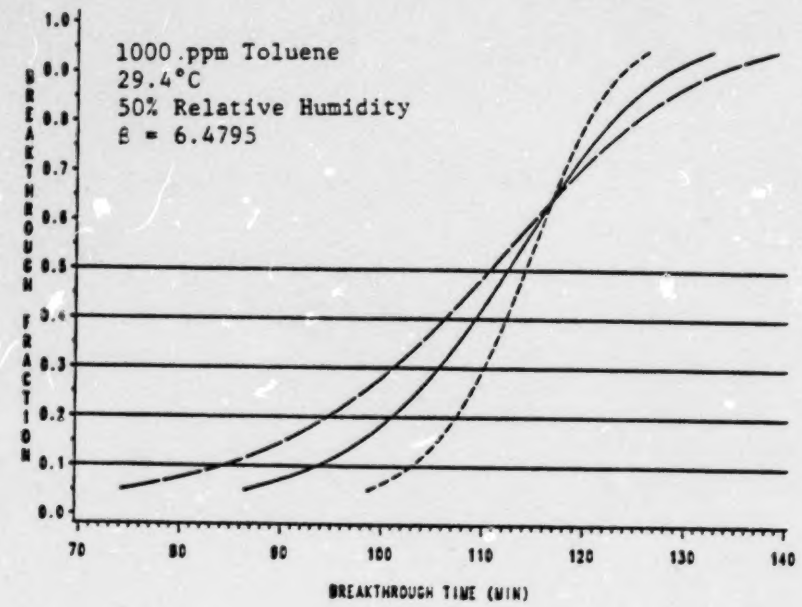

0.6β ------- β ——— 1.4 β — — — —

Figure 1. Effect of parameter β on breakthrough.

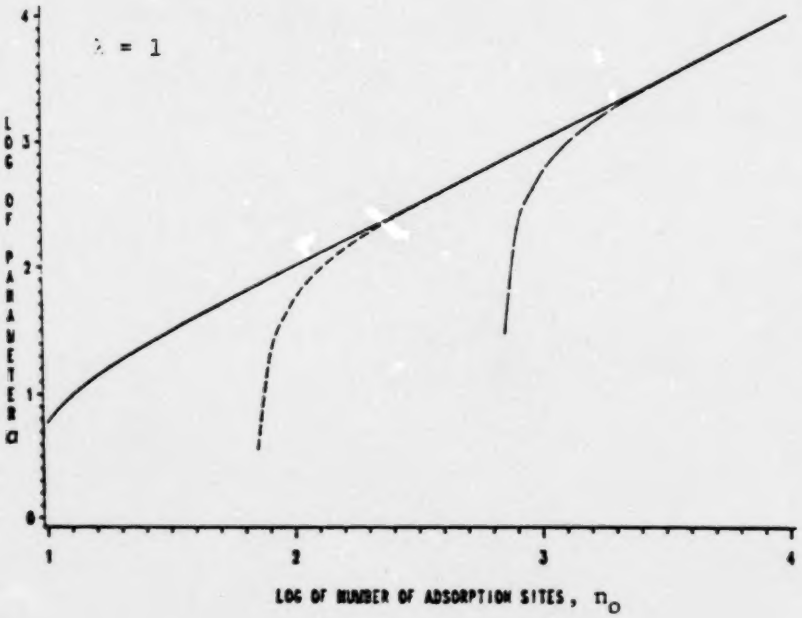

ε = 0.1 ——— ε = 0.01 ------ ε = 0.001 — — —

Figure 2. Convergence of parameter α to n_o.

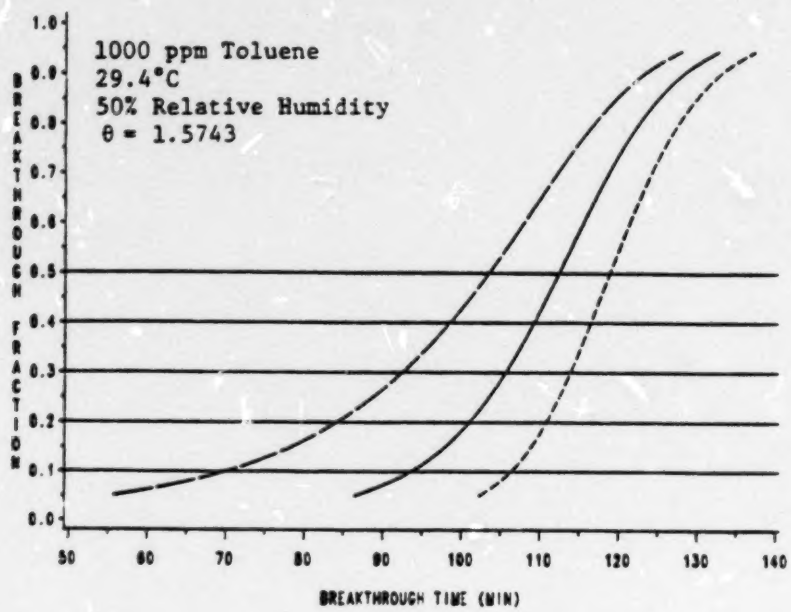

0.5 θ ------ θ ———— 2θ — — — —

Figure 3. Effect of parameter θ on breakthrough.

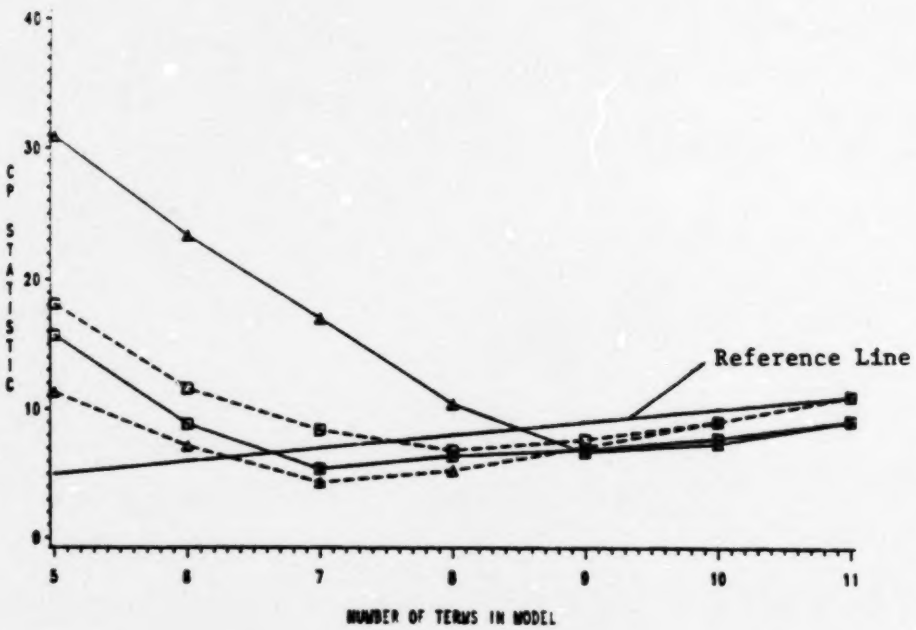

□RH △ABS H HXT ———— NO H X T ------

Figure 4. CP analysis, best subset models for α.

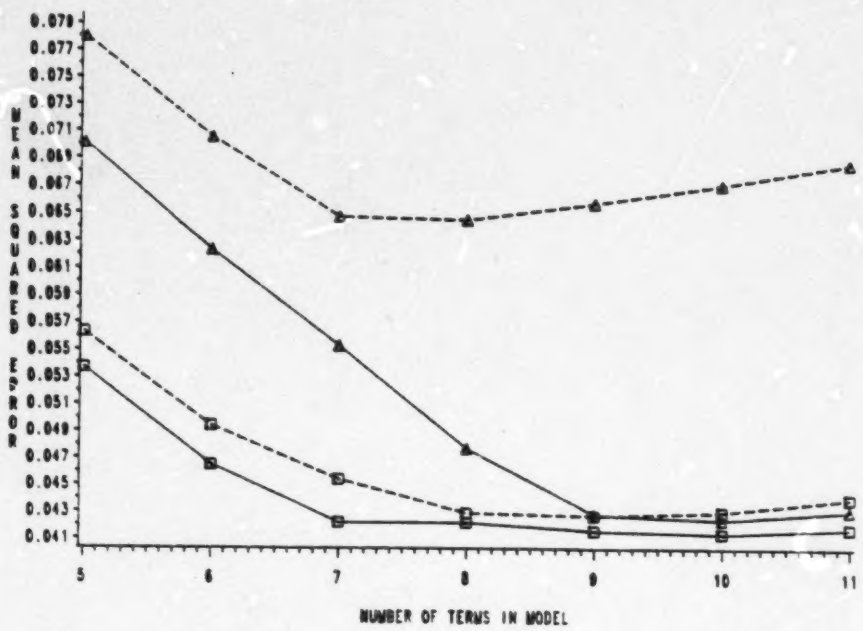

□ RH △ ABS H H X T ——— NO H X T - - - - - -

Figure 5. Mean squared error analysis, best subset models for α.

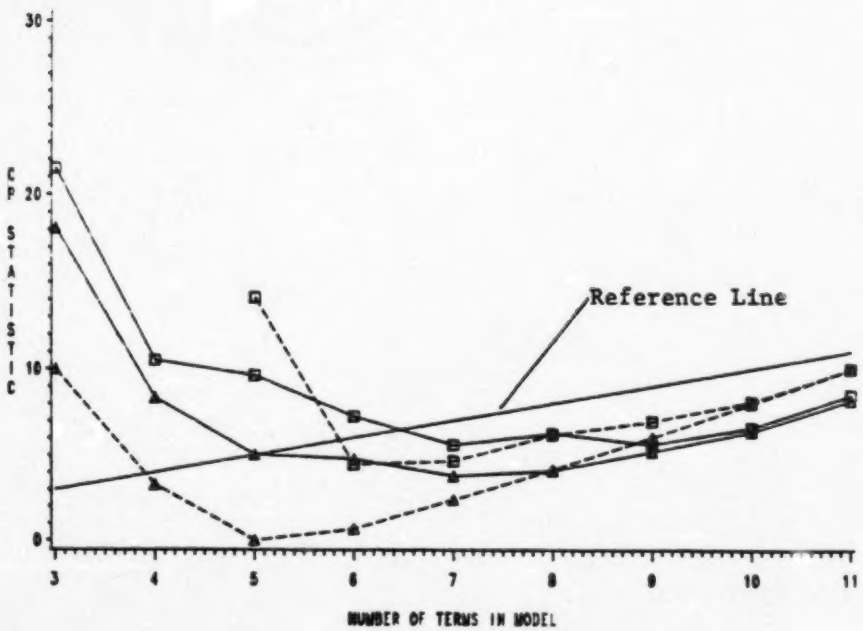

□ RH △ ABS H H X T ——— NO H X T - - - - - -

Figure 6. CP analysis, best subset models for β.

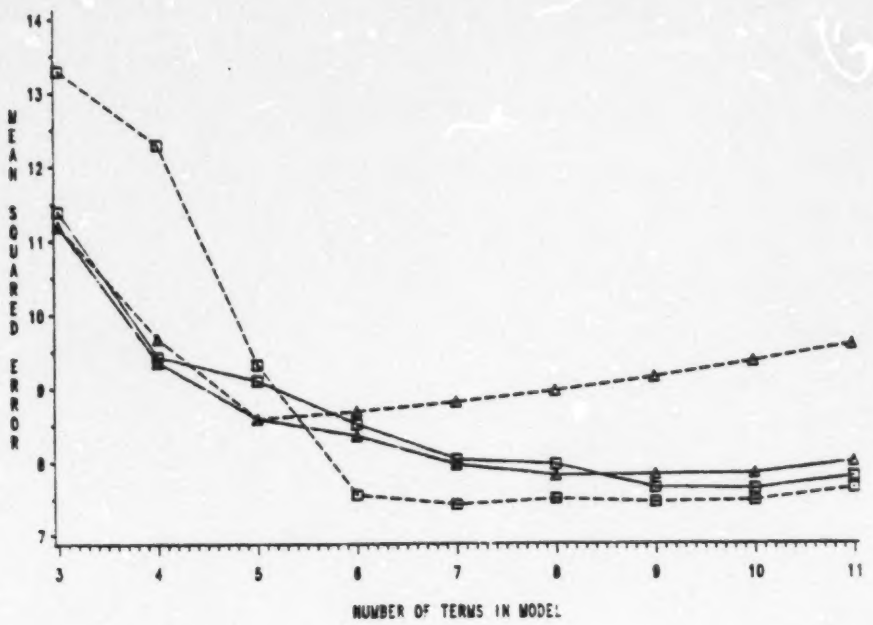

Figure 7. Mean squared error ($x10^{-6}$), best subset models for θ.

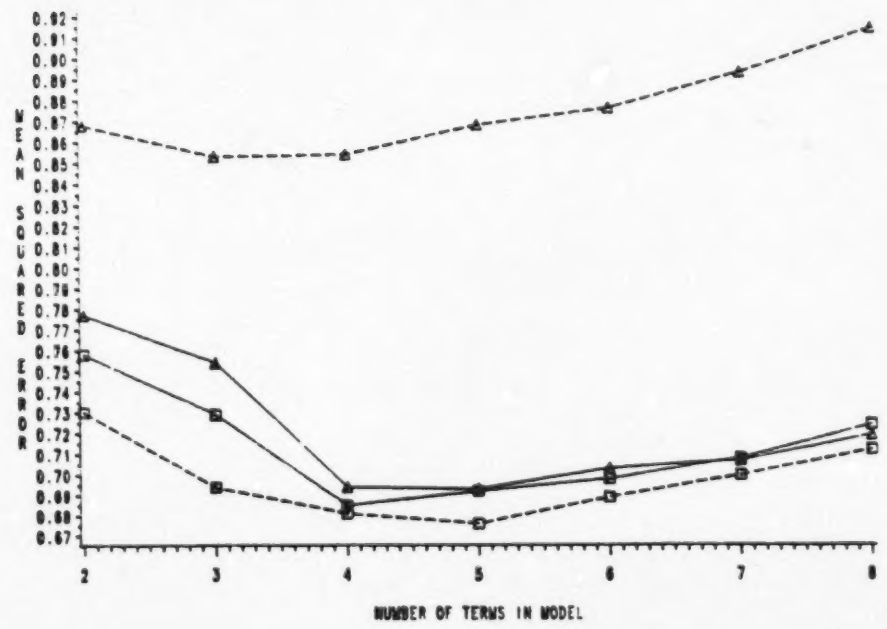

Figure 8. Mean squared error analysis, best subset models for θ.

ACKNOWLEDGEMENTS

An initial form of the PG model (with $\theta = 1$) was suggested by the first author's colleague, Professor Itrel Monroe. Support for this research was provided under U. S. Environmental Protection Agency Cooperative Agreement CR-814945-01-0.

REFERENCES

1. Johnson, N. I. and S. Kotz, Continuous Univariant Distributions-2, Houghton Mifflin Co., Boston, 1970, pp. 1-19.

2. Nunez, C. M., M. Kosusko, and B. E. Daniel, Effect of Humidity on Carbon Adsorption Performance in Removing Organics from Contaminated Air Streams, presented at the 82nd Annual Meeting of the Air and Waste Management Association, Anaheim, CA, June 1989.

3. Draper, N. R. and H. Smith, Applied Regression Analysis, 2nd edition, John Wiley & Sons, New York, 1981, pp. 299-302.